ELSEVIER

Polymer 42 (2001) 7755–7764

polymer

www.elsevier.nl/locate/polymer

Rheo-optics of a conjugated polymer system in shear

Samuel J. Gason[a], Trevor A. Smith[b], David V. Boger[a], Dave E. Dunstan[a,*]

[a]*Co-operative Research Centre for Bioproducts, Department of Chemical Engineering, University of Melbourne, Victoria, 3010, Australia*
[b]*School of Chemistry, University of Melbourne, Victoria, 3010, Australia*

Received 5 January 2001; received in revised form 12 March 2001; accepted 16 March 2001

Abstract

The polymeric chromophore, poly(4-butoxycarbonylmethylurethane), p-4BCMU, has a diacetylene backbone that displays a broad range of optical properties directly attributed to its conformation. The UV-Vis spectral properties of the polymer solution are dependent upon the backbone conjugation length, which describes the length over which the π-electrons are delocalised. The persistence length of the polymer chain describes the curvature of the polymer chain and is dependent upon the solvent quality and thermal properties of the system. Changes in persistence length, which are accompanied by a change in polymer conformation, lead to changes in the conjugation length and, therefore, the measured absorption spectra. However, under an applied shear force, the persistence length of the polymer chain is assumed, through kinetic theories, to remain constant even though the polymer chain may change conformation. A novel rheo-optic experimental system was developed, where a wavelength region of light about the absorption maximum of the polymer backbone is scanned for each shear rate. From the experimental results it was confirmed that while the polymer chain segments aligned in the shear direction, there was no change in the polymer chain persistence length with shear, which is consistent with kinetic theory.

Keywords: Rheooptics; Polydiacetylene; Deformation

1. Introduction

The characteristic optical properties of soluble polydiacetylenes, in particular those with side groups such as nBCMU (butoxycarbonylmethylurethane) offer a unique experimental system in which visible changes in the solution colour may be observed with changing solvent temperature and quality [1–5]. The addition of BCMU side groups to the conjugated polydiacetylene chain forms the polymer soluble in common organic solvents, such as chloroform [6,7].

The soluble polydiacetylenes are understood to undergo conformational changes at different temperatures and in solvents of different quality, leading to changes in the polymer optical properties. The solvato-chromic [1,8–10] and thermo-chromic [11–14] nature of the p-4BCMU polymer chain is characterised by a shift in the solution wavelength of absorption maximum, λ_{max}. The peak at $\lambda \approx 465$ nm, where the solution appears yellow, is characteristic of the polymer in a good solvent. The peak at approximately $\lambda \approx 550$ nm, where the solution appears in the red form, indicates the polymer is in a poor solvent.

The strong absorption spectra of the polymer in the visible region arise from the delocalisation of the π-bonding electrons along the polymer backbone. The observed colour changes are directly attributed to the changes in the backbone from a nonplanar to a planar conformation and hence to changes in the length of electron delocalisation or the conjugation length [15,16]. The change in backbone structure is described as the transition from a random coil chain (yellow solution) to a semi-rod-like polymer structure (red solution). It has been shown by light scattering and UV-Vis spectroscopic measurement techniques that the spectral shift is accompanied by a change in the effective conjugation length of the polymer backbone [15]. Both the above techniques show the polymer to be in the random coil configuration in the good solvent chloroform and a rigid rod configuration in the poor solvent toluene at 25°C.

The shape and size of the random coil in quiescent solution continually fluctuate around the mean value of the radius of gyration. Attempts to describe the instantaneous shape originate from statistical thermodynamics and numerical simulation methods such as Molecular Dynamics or Monte Carlo calculations. Kuhn, in 1934, was the first to show the instantaneous shape of the polymer chain was ellipsoidal and described it as being 'bean-like' [17]. While the individual polymer chains are theoretically

* Corresponding author. Fax: +61-3-8344-4153.
E-mail address: davided@unimelb.edu.au (D.E. Dunstan).

0032-3861/01/$ - see front matter
PII: S0032-3861(01)00227-0

predicted to be ellipsoidal in solution, the macromolecules appear to be spherical when an ensemble average is taken for all orientations in the quiescent state. Additionally, the single macromolecule appears spherical with time due to the conformation fluctuations.

Polymer solutions are often termed complex fluids. Their fascinating and complex range of viscoelastic rheological behaviour includes shear rate dependent viscosity, large storage moduli and significant normal stresses which increase with shear rate [18]. While the elastic dumbbell model is very crude in that it does not include the degrees of freedom or detail the molecular architecture, it may, however, be oriented and is extendable in steady shear. These two characteristics of the dumbbell are essential for the qualitative description of the polymer coil under shear and the steady state rheological properties [18].

More realistic mechanical theories arise from multi-bead models of the polymer chain. Rouse used the simple Stokes-drag law and extended the elastic dumbbell to model the freely jointed bead and spring polymer chain [19]. The coordinated thermal motions of the segments of the polymer molecules cause the configurations to drift towards their most probable distribution under shear [19]. As for the elastic dumbbell model, a probability distribution function for the end-to-end vector may by used to predict the change in chain dimensions for a polymer system under shear. Zimm incorporated the hydrodynamic interactions, including non-free draining and excluded volume, into the Rouse model [20].

In the quiescent state, all molecular orientations are found over the ensemble, therefore, the intrinsic anisotropy in the molecular polarisability does not lead to anisotropy in the material refractive index. If the chain segment is aligned in the direction of flow, its refractive index will depend on relative orientation of the segment to the orientation of the incident light. For a macromolecule under flow, alignment of the optical segments leads to measurable change in the birefringence [21].

The Kuhn and Grun model for a flexible polymer chain relates the statistical integrity of the chain to its optical properties. The flexible polymer chain may be described by a sequence of rigid segments that are interconnected by freely rotating joints. Each segment, defined as a Kuhn segment, has a length and polarisability. The polarisability of the Kuhn segment arises from the polarisability parallel and perpendicular the major axis to the segment. For a cylindrical segment there are two perpendicular polarisabilities which are considered to be equal. The end-to-end vector separating the two ends of the chain arises from the summation of the vectors describing the orientation of each polymer segment. The polarisability of the entire chain is therefore the sum of the polarisability of the segments taking into account each segment orientation.

The average probability distribution describing the end-to-end vector as a function of the segment orientation was given by Kuhn and Grun [22]. From the distribution, which contains the Langevin function, the average end-to-end tensor may be used to predict the anisotropic part of the polarisability of the polymer chain. Changes in end-to-end vector may be predicted from the models for the dynamic properties of polymers in solution. The polarisability is then related to the refractive index tensor of the polymer chain. The anisotropy in the refractive index induced by shear may be measured and directly related to changes within the polymer chains. Further derivations and discussion on the Kuhn and Grun model may be found in the texts by Treloar and Fuller [22,23].

Peterlin, Heller and Nakagawa first highlighted the potential use of optical techniques in the characterisation of polymer response to flow [24]. The angle of the longest axis for the deformed (ellipsoid) gyration space and the three main radii of molecular gyration of the deformed polymer could be measured by light scattering. The measurement of these two physical properties allows for the elucidation of the hydrodynamic orientation and deformation of the polymer chain.

Cottrell et al. experimentally measured the polymer (polyisobutylene, PIB in decalin) orientation and deformation due to shear using light scattering techniques [25]. The degree of deformation of the actual polymer chain is then inferred from the experimentally measured change in radius of gyration of the volume enveloping the polymer. More recently, work by Springer and co-workers, [26,27] and Muller and co-workers [28,29] on polystyrene systems has confirmed the results of Cottrell et al. Predictions of the polystyrene coil deformation relevant to the flow light scattering experiment have been presented by Li et al. [30]. The results obtained by Cottrell et al., Springer et al. and Muller et al. show that large discrepancies exist between the theoretical predictions of Rouse-Zimm and the experimental data for polymer behaviour under shear [23,26]. Bossart and Ottinger have also recently improved the Zimm polymer theory leading to a better correlation between the flow birefringence and scattering experiments of polymer coils in dilute solution and kinetic polymer theory [31].

Recent rheo-optic experiments by Chu and co-workers have directly observed, with video fluorescence microscopy, the deformation and alignment of individual DNA coils under shear [32,33]. The probability distribution function for the molecular extension was determined as a function of shear rate for two different polymer relaxation times. In contrast to pure elongation flow, the average polymer extension does not show a distinct coil-stretch transition. The coil shows large temporal fluctuations consistent with end-over-end tumbling of the molecule [32].

As previously discussed, large discrepancies are seen between the flow light scattering data and the theoretical Rouse-Zimm predictions of the polystyrene coil deformation [25]. However, the experimental observations of the DNA orientation have successfully been compared with the finitely extensible dumbbell model and the Rouse-Zimm

model of the polymer coil [32]. Li and Larson present a comprehensive discussion of the flow light scattering and DNA flow visualisation experiment [32]. While both experimental systems are unique, a comparison has been made between the two systems for the overall deformation of the polymer coil by the 'expansion ratio'. The deformation or expansion of the DNA was shown to be significantly larger than the deformation of the polystyrene coil. Three possible explanations of this discrepancy are presented and are further discussed [32].

The rheo-optic measurements of polydiacetylenes under shear have been undertaken in this study in order to quantify changes in the conjugation length of the polymer in shear. The polymer has been shown to be a random coil in chloroform solution consistent with prior studies using light scattering [1]. Results are presented for the p-4BCMU in three different solvent conditions.

2. Experimental section

2.1. Characterisation

The p-4BCMU used in this study was synthesised following literature procedures [34]. The polymerisation was achieved using γ-ray (^{60}Co) irradiation. GPC-light scattering employing a Dawn Wyatt system was used to measure the molecular weight and polydispersity of the polymer in tetrahydrofuran, THF. The synthesised p-4BCMU has a M_w of 800 kg/mol with a polydispersity of 1.8 (M_w/M_n) and the radius of gyration, $\langle s^2\rangle^{1/2}$, was found to be approximately 42 nm.

Ultra-Violet Visible (UV-Vis) absorbance spectra were collected using a Cary 3E UV-Vis Spectrophotometer over a wavelength range of 300–600 nm. The intrinsic viscosity, [η], of the p-4BCMU in chloroform and chloroform-dioctyl phthalate was measured using the Schott AVS 350 automated viscosity measuring unit with Ubbelohde capillary viscometers.

2.2. Rheo-optic measurements

The spectroscopic technique employed uses quartz concentric cylinders as described elsewhere [35]. The ratio of the radii of the two glass cylinders is greater than 0.95 and this ensures that a nearly constant shear rate is maintained across the gap. The Couette cell is placed in the Cary 3E Spectrophotometer and manually adjusted so that the flow field is perpendicular to the incident beam. Calculation of the Taylor number showed that at the maximum shear rates attained in this study there would be no recirculation zones present [36]. The incident beam was also polarised using a Melles Griot prism polariser orientated either parallel or perpendicular to the flow field allowing absorbance changes in either direction to be recorded.

Spectra were collected with shear rates varying from 0 to 2000 s^{-1}. The spectra were normalised by dividing the difference between the shear and quiescent spectra, by the quiescent spectra. The change in absorbance, ΔAbs, at a given wavelength, due to shear, is calculated using Eq. (1):

$$\Delta\mathrm{Abs} = \frac{A_{\mathrm{Shr}} - \frac{(A_{\mathrm{Pre}} + A_{\mathrm{Post}})}{2}}{\frac{(A_{\mathrm{Pre}} + A_{\mathrm{Post}})}{2}} \tag{1}$$

where A_{Pre} is the average pre-shear absorbance, A_{Post} is the post-shear absorbance and A_{Shr} is the shear absorbance. The reduced change in extinction coefficient, $\Delta\epsilon$ may be calculated by use of the Beer Lambert Law, where Abs. $= \epsilon.l.c$, where l and c are the path length and concentration respectively. All measured changes in the extinction coefficient with shear were reversible.

The deformation and orientation of the polymer chain subjected to a shear force may be predicted as a function of the reduced shear rate, β. When subjected to shear flow the state of the polymer macromolecules is governed by the competition between the randomising effect of the thermal motion of the molecular segments and the hydrodynamic force of shear inducing alignment of the molecule. In the quiescent state a polymer molecule is free to rotate and translate due to Brownian motion. Upon the application of a shear field, hydrodynamic forces are superimposed on the rotational and translational diffusion forces on the polymer coil. When the hydrodynamic forces begin to dominate the Brownian forces, spatial organisation of the chain segments and deformation of the polymer occurs. Thermal Brownian motion tends to randomise the orientation of the molecules, thereby opposing the alignment. The balance between the opposing effects of hydrodynamic and Brownian forces is characterised by the product of the characteristic relaxation time, τ, and the time-scale of the experiment and is defined as the *reduced shear rate*, β. The polymer molecule is predicted to deform for $\beta > 1$ [26]. In the present case β is defined by:

$$\beta = \tau \cdot \dot{\gamma} \tag{2}$$

where $\dot{\gamma}$ is the shear rate and the characteristic relaxation time, τ, is defined as:

$$\tau = \frac{[\eta]\eta_s M_w}{kT} \tag{3}$$

where [η] is the polymer intrinsic viscosity, η_s the solvent viscosity, M_w is the molar mass, k and T have their usual meanings.

3. Results and discussion

3.1. Optical characterisation of p-4BCMU

The spectral properties of the p-4BCMU in the different solvent systems were measured between 300 and 600 nm.

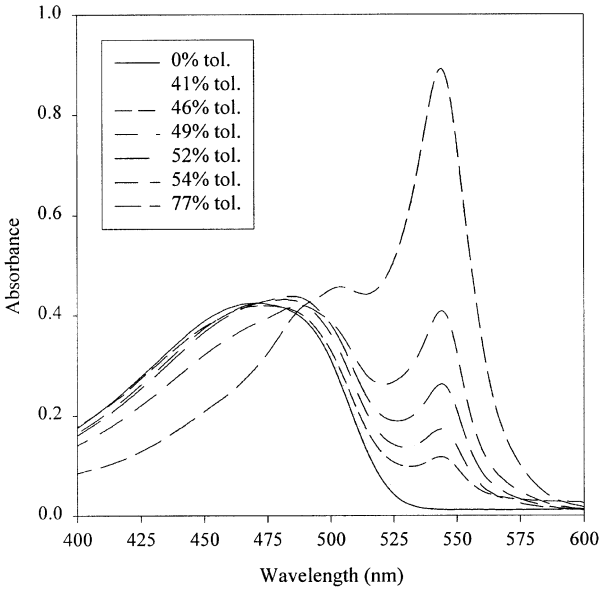

Fig. 1. UV-Vis optical absorption spectrum of p-4BCMU in solution (0.03 g/L). The polymer, p4BCMU, in chloroform (yellow form) has the peak at 468 nm and in $CHCl_3$-Tol (red form) has the peak at 545 nm.

The UV-Vis spectrum, shown in Fig. 1, highlights the transition in λ_{max} from 468 nm for p-4BCMU in the yellow form to 550 nm for the red form. An isobestic point is shown to occur at a wavelength of approximately 490 nm. The solvato-chromic spectral transition observed is characteristic of the p-4BCMU sample. The extinction coefficient, ϵ, was experimentally measured at $\lambda = 468$ nm for the p-4BCMU in $CHCl_3$ and found to be $3.55 \times 10^5\ M^{-1}\ cm^{-1}$. The extinction coefficient for the $CHCl_3$-Tol system at $\lambda = 550$ nm was calculated as $4.75 \times 10^5\ M^{-1}\ cm^{-1}$. The difference in extinction coefficient between the two forms arises from the differences in the molecular structure in the good/poor solvents. The polymer has been shown to be in the random coil configuration in the good solvent, $CHCl_3$, and rod-like in the poor solvent toluene. In toluene the distribution of conjugation lengths is narrower and therefore the extinction coefficient at $\lambda = 550$ nm is larger.

3.2. Conjugation length and persistence length

Two different structural models, have been used to describe the polydiacetylene chain. The Kuhn model describes the chain as a series of planar segments broken up by 90° rotations about the backbone. The conjugation length is then used to describe the length of each segment. The Porod-Kratky, 'worm-like', model describes the chain as being continuous and smooth where each bond is slightly twisted, maintaining the chain curvature. The statistical segments (persistence length) of the 'worm-like' chain are shown to be of greater length than the Kuhn model [10,13].

Patel and Miller used quantum mechanical calculations to predict the average conjugation length of the polymer chain in the red and yellow form [37]. The energy of the light absorbed is related to the conjugation length over which the delocalised π-electrons are able to travel unperturbed. The formulation of the relationship between the number of conjugated bonds, l_{ec}, and the energy of the absorbance maximum (bandgap), E_g, relies upon the poly(diacetylene) chain being analogous to the chain of the polyenes [14].

$$E_g = V_0 + \left(\frac{h^2}{4m_e(l_m/2)^2} - \frac{V_0}{4} \right) \frac{1}{(l_{ec} + 0.5)} \tag{4}$$

where V_0 is understood to be the amplitude of a sinusoidal potential which corrects the free energy electron gas model for bond length alteration and has a value of 1.75 eV for the system used in this study [14]. h is Planck's constant, m_e is the mass of the electron and l_m is the length of one monomer unit ($l_m = 5$ Å). The values obtained from this analysis are $8 > l_{ec} > 6$ repeat units for the random coil yellow form and $20 > l_{ec} > 10$ repeat units for the rod like red form, as seen in the figure. Simple division of the absorbance wavelengths associated with each form of the polymer yields a 7 nm shift in the absorption wavelength for a change of one repeat unit in the conjugation length [38–40]. Such a spectral shift would be readily measurable with the apparatus used in this study.

The UV-Vis spectrum of p-4BCMU in solution is, therefore, essentially a measure of the distribution of conjugation lengths for the polymer chain. Any change in the distribution of conjugation lengths should result in a deviation in the first differential of the absorption spectrum with the light wavelength, $\Delta Abs/\Delta\lambda$. The spectrum was differentiated by a floating three-point differentiation. The first differential is also equal to zero at the λ_{max} for p-4BCMU in chloroform and for p-4BCMU in chloroform-toluene, as shown in Fig. 2(a). When the solvent quality for the polymer solution is changed from 'good' to 'poor' there is a dramatic change in the first differential of the absorption spectrum, as shown in Fig. 2(a). Therefore, differentiation of the spectrum provides an accurate method of detecting the induced conformation and conjugation length changes in the polymer system.

Dioctyl phthalate was added to the system to increase the solvent viscosity and as a 'poor' solvent it would be expected to have some effect on the polymer UV-Vis absorbance spectrum. Even though the absorbance maxima in the ($CHCl_3$-DOP) system and the pure chloroform system are the same ($\Delta Abs/\Delta\lambda = 0$ at $\lambda_{max} = 468$ nm), subtle changes in the spectra are seen. Differentiation of the p-4BCMU in $CHCl_3$ spectra and the p-4BCMU in $CHCl_3$-DOP spectra results in a small shift in the peak at approximately $\lambda = 510$ nm. This indicates that while the median conjugation length (and therefore λ_{max}) remain constant, a slight increase in the number of longer conjugation length segments is observed, Fig. 2(b).

3.3. Rheological characterisation

The intrinsic viscosity of the p-4BCMU was found in

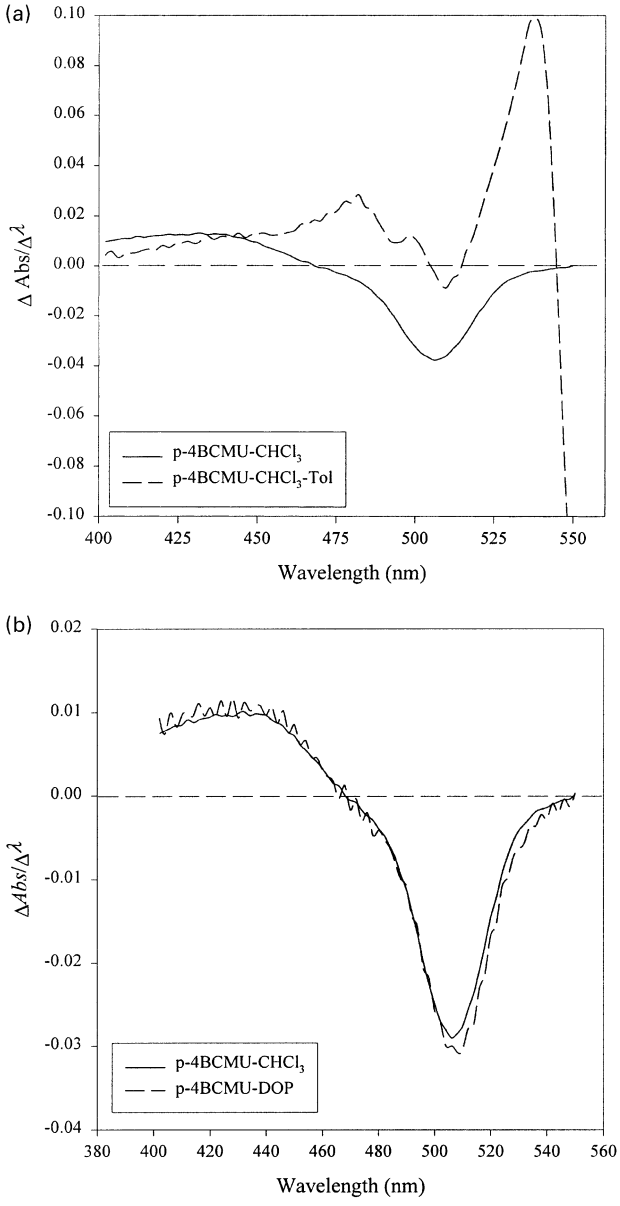

Fig. 2(a). The first differential of the UV-Vis optical absorption spectrum of p-4BCMU (2.25 g/l) in $CHCl_3$ (yellow form) and (2.25 g/l) in $CHCl_3$-Tol (red form) (77 wt% toluene) and (b) The first differential of the UV-Vis optical absorption spectrum of p-4BCMU in $CHCl_3$ and in $CHCl_3$-DOP. (p-4BCMU at 2.25 g/l and 30 wt%DOP).

chloroform (300 ml/g), chloroform-dioctyl phthalate (275 ml/g) and chloroform-toluene (130 ml/g) at 25°C. The Mark-Houwink equation may be used to relate the intrinsic viscosity to the molecular weight by the viscosity constant, K_η, and the exponent, a_η. The Mark-Houwink parameters have been reported as $K_\eta = 1.05 \times 10^{-2}$ and $a_\eta = 0.83$ for p-4BCMU, in $CHCl_3$ at 25°C [41,42]. Using these Mark-Houwink parameters gives a viscosity molecular weight, M_η, of approximately 5×10^5 g mol^{-1}. The exponent a_η describes the state of the polymer in the given solvent. For a polymer in a theta solvent, the exponent a_η has a value of approximately 0.5, whereas in a good solvent it is larger and may be as high as 0.8 as seen in this system, further evidence of the p-4BCMU adopting a random coil configuration in chloroform [41]. The intrinsic viscosity of the p-4BCMU is reduced with the addition of a poor solvent. This is consistent with the contraction and subsequent reduction in volume of the polymer chain [42,43].

The critical overlap concentration, c^*, which may be approximated from the intrinsic viscosity experiments, describes the polymer concentration where the individual polymer chains begin to interact in solution. More specifically, the polymer/solvent concentration inside the coil is equal to that of the polymer coil in bulk solution. The overlap concentration may be approximated as the concentration corresponding to the transition from the kinematic viscosity $\sim c - \sim c^3 - ^4$. The c^* for the p-4BCMU in chloroform at 25°C was found to be approximately 0.007 g/ml (0.46 wt.%).

3.4. Rheo-optic measurements on p-4BCMU solutions

The spectral changes induced in the polymer in different solvent conditions are shown in Fig. 1 where the spectra are shown for a range of toluene/chloroform mixtures. The thermo-chromic behaviour has been reported elsewhere [44].

3.5. Chloroform solutions

Absorbance spectra under various shear conditions were collected using unpolarised light for solutions of p-4BCMU in chloroform over the wavelength range (300–600 nm). Firstly, an absorption spectrum was collected without shear and taken as the experimental baseline. Shear was then applied to the sample and the spectra collected, as shown in Fig. 3. The sample was allowed to stand unperturbed and another spectrum was then recorded, indicating that the sample had returned to its original quiescent state. The spectral changes between the initial and sheared state were then used to quantify the induced anisotropy in the polymer solution. Fig. 3 shows the unperturbed and shear ($\dot{\gamma} = 2000$ s^{-1}) spectra for the test solutions of different p-4BCMU concentrations in $CHCl_3$. In each experiment the measured absorbance was seen to increase with shear. This is further highlighted by Fig. 4, which shows the shear-UV-Vis spectra for 2.25 mg/ml p-4BCMU in chloroform for the range of shear rates shown.

The UV-Vis absorption spectrum is essentially a measure of the polymer persistence length distribution. Any changes in the polymer persistence length distribution, such as those seen with the solvato-chromic and thermo-chromic changes, would give rise to significant differences between the first derivative of the absorbance spectra for p-4BCMU under shear and the quiescent state.

While a change in the persistence length would be expected to produce a difference in the spectra differentiation, it may not result in a change in the actual absorbance

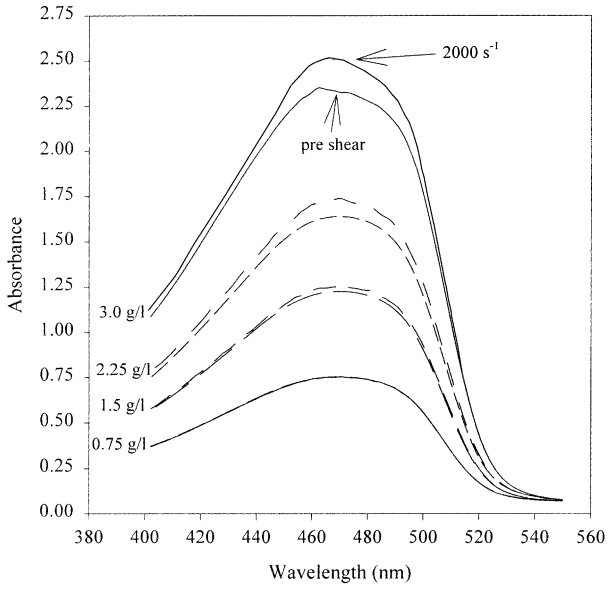

Fig. 3. Measured shear spectra for four different concentrations shown of p-4BCMU in $CHCl_3$. The lower curve of each set is the pre shear baseline and the upper curve is the shear spectra (at 2000 s^{-1}). While there is an increase in absorbance for all solutions, there is no measured change in λ_{max}.

maximum, λ_{max}. No shift in λ_{max} was observed for the p-4BCMU in the shear field up to the highest shear rates attainable, as $\Delta Abs/\Delta\lambda = 0$ at $\lambda = 468$ nm for both the quiescent and shear spectra, Fig. 5(a). Also there is no distortion of the persistence length distribution function as there is no shear-induced deviation in $\Delta Abs/\Delta\lambda$. Differentiation of the p-4BCMU-Tol solution spectrum is also given in Fig. 5(a) as a reference for a measured change in the

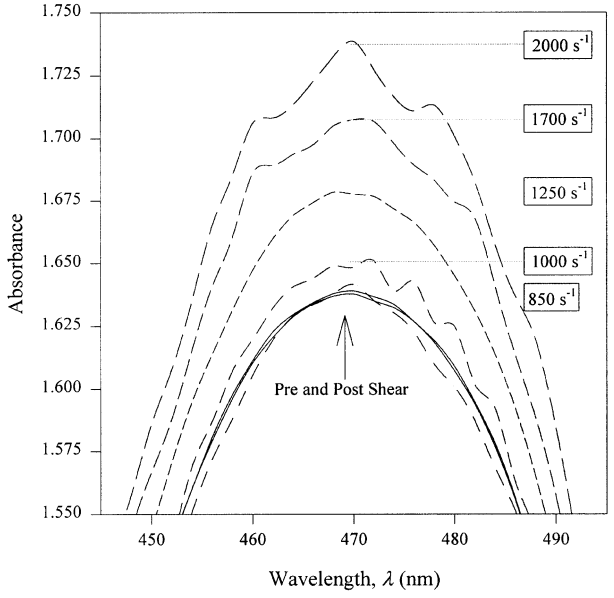

Fig. 4. Shear spectra for 2.25 mg/ml p-4BCMU in $CHCl_3$. The lower curve is the pre shear and post shear. The shear rate at which each spectrum is collected is given. While there is an increase in absorbance for all solutions, there is no measurable change in λ_{max} with shear.

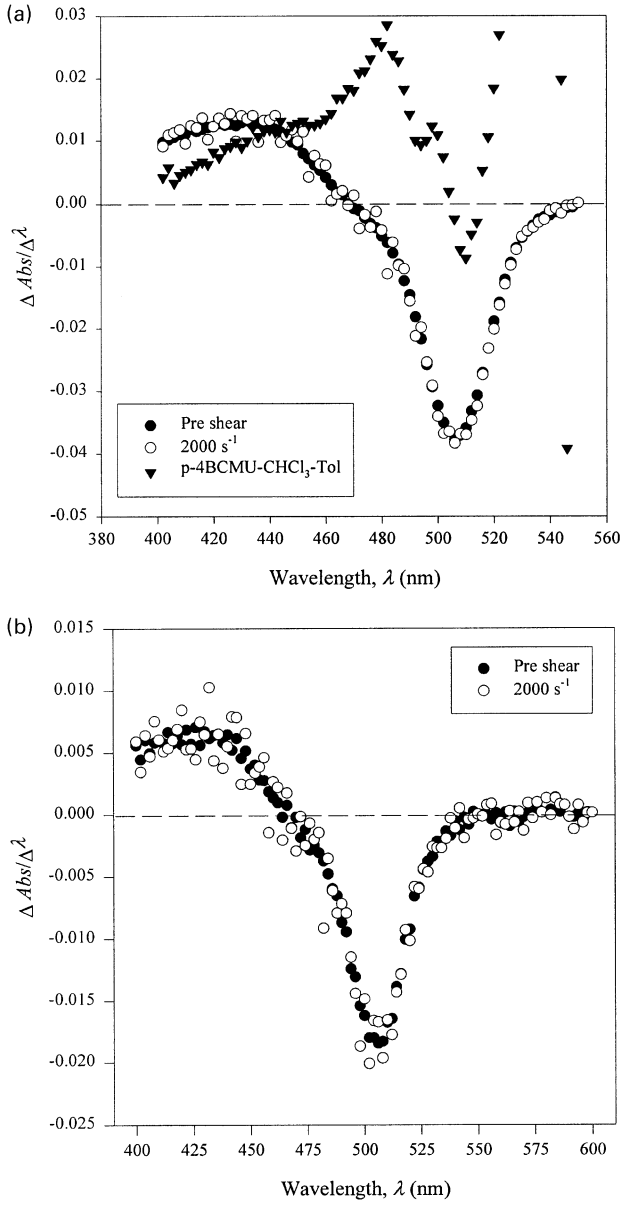

Fig. 5. (a) Differentiation of the shear spectrum for 3.0 mg/ml p-4BCMU in $CHCl_3$ and (b) Differentiation of the shear spectrum for 3.0 mg/ml p-4BCMU in $CHCl_3$-DOP (30 wt%DOP).

polymer persistence length. Given the nature of the spectral changes observed with differing solvent quality and temperature, it may be concluded that the shear field induces no observable distortion of the macromolecule persistence length.

The Beer Lambert law is used to calculate the extinction coefficient, ϵ, of the molecules and can be directly employed to interpret changes in the absorbance and relate them to the induced anisotropy of the polymer molecules. Given the constant concentration and path length used in the experiments, the change in absorbance spectra may, therefore, be interpreted as a change in the extinction coefficient. The change in extinction coefficient with shear, yields a change in the extinction cross-sectional

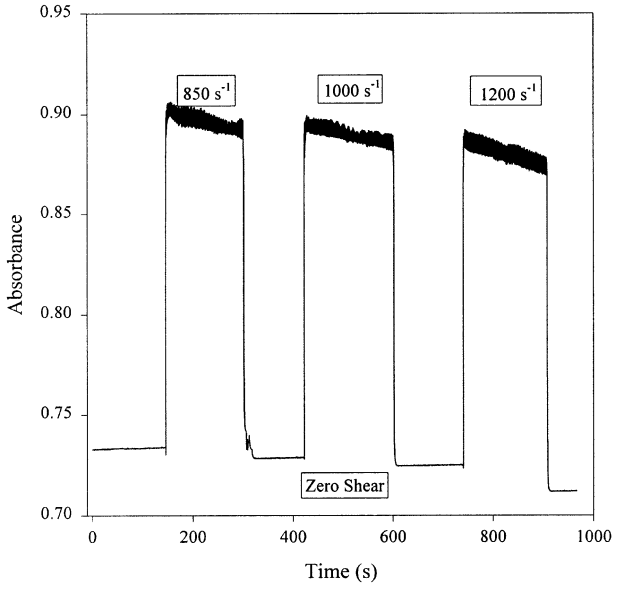

Fig. 6. Measured absorbance versus time for 3.0 mg/ml p-4BCMU in $CHCl_3$-Tol (77 wt% toluene) at $\lambda_{max} = 550$ nm. The absorbance is shown to increase upon the application of shear at the shear rates given.

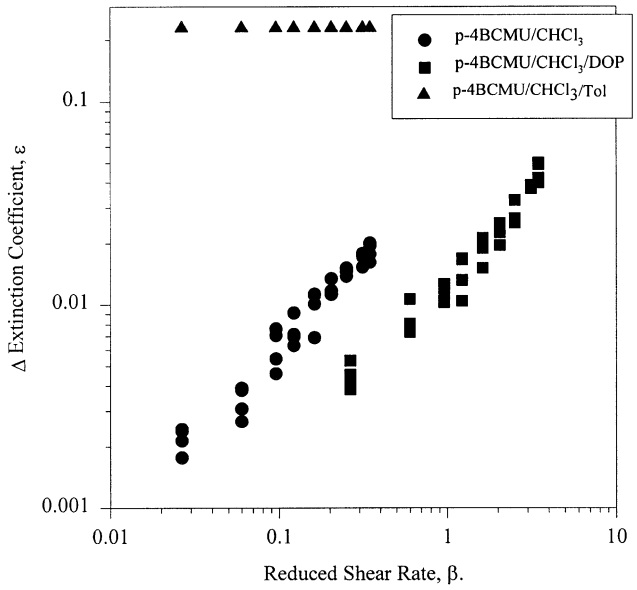

Fig. 7. Change in extinction coefficient, $\Delta\epsilon$, at λ_{max} versus the reduced shear rate, β, for the $CHCl_3$ and the $CHCl_3$-DOP (30 wt% DOP) systems for the four test solution concentrations. There was no concentration dependence on the $\Delta\epsilon$ with shear.

surface area of the molecule incident to the light beam, at any given shear rate. The change in extinction coefficient may thus be attributed to the ordering of the absorbing chain segments relative to the light beam. The observed shear spectrum changes were reversible and time independent, indicating that changes seen were shear-induced and did not originate from variations in concentration and temperature.

3.6. Chloroform-dioctyl phthalate solutions

The solvent viscosity was increased by the addition of dioctyl phthalate, and, therefore, the characteristic relaxation time of the polymer in solution was increased. As previously mentioned the addition of dioctyl phthalate to the p-4BCMU-$CHCl_3$ solution reduces the solvent quality, thereby slightly reducing the flexibility of the chain. Upon application of shear to the system it is observed that the change in absorbance has the same characteristics as the chloroform solution, where no change in λ_{max} with shear is observed, Fig. 5(b). Therefore, as with the p-4BCMU in $CHCl_3$ experiment, the persistence length of p-4BCMU in $CHCl_3$-DOP remains unchanged with shear.

3.7. Chloroform-toluene solutions

Adding toluene to a chloroform solution (3:8 v$CHCl_3$/vTol) induced the rigid rod (red) form of p-4BCMU. Flow spectra using the same protocol as described above were collected and show a large increase in the extinction coefficient and no change in λ_{max}. Additionally, the change in the extinction coefficient, $\Delta\epsilon$, was observed to be independent of shear rate over the range for the p-4BCMU-Tol solutions, as shown in Fig. 6.

The change in absorbance, ΔAbs, at λ_{max} due to shear for the p-4BCMU in $CHCl_3$ and $CHCl_3$-DOP is characterised by quantification of the absorbance differences. Therefore, by use of the Beer Lambert law, where Abs. $\propto \epsilon$, the reduced change in absorbance value will be the same as that for the reduced change in extinction coefficient, $\Delta\epsilon$, Eq. (1). The change in extinction coefficient, $\Delta\epsilon$, increases with shear rate for the $CHCl_3$ and DOP-$CHCl_3$ systems, as shown in Fig. 7.

The alignment of the p-4BCMU molecules as determined by the change in the extinction coefficient versus shear rate, shows an interesting trend. For p-4BCMU in the poor solvent toluene, dramatic alignment occurs at very low shear rates after which the degree of alignment is constant with shear. The measured change in extinction coefficient is also very large. The $CHCl_3$-DOP system shows a smaller change in extinction coefficient with shear than the pure chloroform system indicating that the alignment is greater for a given reduced shear rate in the better solvent. This is in contrast to the observation for the toluene system.

3.8. Polarisation experiments

The symmetry of the experimental system enables absorption spectra both parallel and perpendicular to the direction of the shear to be measured. The change in extinction coefficient was found to be positive for light polarised parallel to the shear direction and negative for light polarised perpendicular to the shear direction. The changes in the extinction coefficient are independent of concentration at a shear rate of 2000 s^{-1}. This observation is consistent with changes observed using the unpolarised incident beam.

Table 1
The change in extinction coefficient, $\Delta\epsilon$, for p-4BCMU in $CHCl_3$ under shear using polarised light. The angle of polarisation to the shear direction is given. The dichroic ratio from the $\Delta\epsilon$ data is also presented

Polarisation	Shear rate (s^{-1})	Change in extinction coefficient, $\Delta\epsilon$		
		$CHCl_3$	$CHCl_3$-DOP	$CHCl_3$-Tol
None	150–2000	Fig. 7	Fig. 7	0.229
0°($\|\|\gamma$)	2000	0.015	0.032	0.294
90°($\top\gamma$)	2000	−0.009	−0.020	−0.052
$\Delta\epsilon_{\|\|}/\Delta\epsilon_{\top}$	2000	1.7	1.6	5.6

Importantly, the extinction coefficient for the p-4BCMU-$CHCl_3$-Tol solutions increases for light polarised parallel to the shear flow, and decreases for light perpendicular to the flow, as observed for the p-4BCMU-$CHCl_3$ and p-4BCMU-$CHCl_3$-DOP systems. For the p-4BCMU-$CHCl_3$-Tol solution no change in the $\Delta\epsilon$ was observed for shear rates above 150 s^{-1}, suggesting that the polymer is in its maximum aligned state.

The dichroic ratio, $\Delta\epsilon_{\|}/\Delta\epsilon_{\top}$, is related to the polarisability of the polymer chain. The dichroic ratio for p-4BCMU in the various solvent conditions (Table 1) highlights the effect of solvent quality on the conjugation length. For p-4BCMU in a good solvent such as $CHCl_3$, the dichroic ratio of the conjugated backbone is close to unity, but does show that the extinction of the light polarised parallel to the backbone is greater than the extinction of light polarised perpendicular to the backbone. For p-4BCMU in a $CHCl_3$-Tol solution, where the polymer is more rod-like and shown to have a longer conjugation length, the dichroic ratio of the polymer backbone is dramatically increased, Table 1. The increase in the number of monomer segments in the conjugation length of the polymer in poor solvent, gives rise to the increase in the extinction of light parallel to the polymer backbone, compared to the polymer backbone in a good solvent.

As previously shown the p-4BCMU in a good solvent has a conjugation length comprising of six to eight monomer units. Upon the addition of a poor solvent, the number of monomer units in the conjugation length increases from between 10 and 20 monomer units. The increase in the dichroic ratio for the polymer backbone when in poor solvent compared to a good solvent is therefore, directly related to the increase in the number of monomer units in the conjugation length. The dichroic ratios measured in this study, as shown in Table 1, closely correspond to the polarisability ratio, $\alpha_1/\alpha_2 \cong 1.4$ for p-4BCMU in $CHCl_3$ as measured by Chance et al. [41]. Heeger used electric birefringence to measure response and anisotropy of a p-4BCMU in the poor solvent to be 600 times greater than that for the p-4BCMU in the good solvent [45]. Due to the inherent differences in experimental systems it is not feasible to quantitatively compare the measured changes in extinction by Heeger to the changes in extinction described in this study. However, using shear spectroscopy it may be shown that the difference in $\Delta\epsilon$ for p-4BCMU in good and poor solvents is significantly large.

The experimental data obtained for p-4BCMU in the three different solvents may be summarised as follows: no spectral change occurs as the shear rate is increased, while ϵ increases parallel and decreases perpendicular to the shear field. Given the sensitivity of the spectra to changes in the conjugation length and that no spectral shift is observed up to the highest shear rates attainable, no change in the average conjugation length and therefore no change in the persistence length of the polymer is induced by the shear field. While there is no change in the persistence length of the polymer backbone, change in the end-to-end distance in the shear field up to the highest shear rates used in these experiments is observed as an increase in the polymer extinction coefficient with shear.

3.9. Alignment of the polymer chain

The description of the polymer coil as a chain of connected 'blobs' arose from the crossover between Gaussian chain statistics and the excluded volume effects observed in the intrinsic viscosity, [η], measurements [46]. In the model, the macromolecular chain is comprised of N/N_c blobs, where N is the number of statistical segments in the chain and N_c is the number of statistical segments in one blob [47]. Polymer 'blob' theory of the chain predicts the macromolecule within the 'blob' obeys Gaussian statistics, while excluded volume effects are taken into account over the entire chain. The viscometric expansion factor, α_η, combines the relation for blob theory by de Gennes and the dynamic arguments of Weill and des Cloizeaux [46,48].

$$\alpha_\eta^3 = \frac{[4(1-\upsilon)(2-\upsilon)]}{[(2\upsilon+1)(\upsilon+1)]}\left(\frac{N}{N_c}\right)^{3\upsilon-1.5} \tag{5}$$

$$a_\eta = 3\upsilon - 1 \tag{6}$$

where υ is the excluded volume index and a_η is the Mark-Houwink exponent. Dondos presented the experimental relationship between the N_c and the Mark-Houwink exponent, a_η, where N_c may be related to any polymer system for the given value of a_η, Eq. (7) [49].

$$N_c = 0.37\ \alpha_\eta^{-7.7} \tag{7}$$

The 'blob' model uses features of the random flight chain, including the contour length, L, monomer length, l_m, number of monomers, n_m, and the intrinsic properties to predict the dimensions of the blobs in the chain. The number of statistical segments within one blob, N_c, calculated from the empirical relationship given in Eq. (6) was found to be 3.4 for p-4BCMU in $CHCl_3$ [47]. For the case of the p-4BCMU in $CHCl_3$ the persistence length, p_l ($\cong$ 4.5 nm). Therefore, the number of segments and the number of blobs for the entire chain, $N = L/p_l \cong 262.33$ and $N/N_c \cong 75$. The blob diameter, ξ_b, and the chain dimensions end-to-end distance,

r_b, and the radius of gyration, s_b, are given by Rieger as:

$$\xi_b^2 = l_m^2\left(\frac{p_l}{l_m}\right)^{2\upsilon} \tag{8}$$

$$r_b^2(N,\upsilon) = n_m^{2\nu} l_m^2 \frac{\Gamma(N+1)\Gamma(2\upsilon+1)}{\Gamma(2\upsilon+N)} \tag{9}$$

$$s_b^2(N,\upsilon) = n_m^{2\upsilon}\frac{l_m^2}{6}\frac{\Gamma(N+3)\Gamma(2\upsilon+1)}{\Gamma(2\upsilon+2+N)} = \frac{r_b^2(N+2\upsilon)}{6} \tag{10}$$

where γ is the gamma function [50]. The blob diameter, or the correlation length, ξ_b, calculated from Eq. (8), was found to be approximately 3.75 nm. This value is dependent upon the method used to calculate the persistence length. The overall chain dimensions may be calculated from the blob model using the viscometric expansion factor calculated by Eq. (5), $\alpha_\pi^3 = 2.34$ [50,51]. The end-to-end distance, r_b, and the radius of gyration, s_b, were found to be 34.3 and 36.5 nm respectively. The radius of gyration for the p-4BCMU chain calculated using 'blob' theory is consistent with the values experimentally measured value of 42 nm.

The internal structure of each blob, in the quiescent and sheared state, is continually changing due to thermodynamic motion. When a shear force is applied to the polymer system the perturbed blob chain will rearrange from the quiescent state. While the overall motion of the 'blob' chain is altered by a shear induced deformation, the size and shape of each blob and the chain persistence length remain constant. The shear-induced perturbation on the polymer-blob system will occur by rotation about the bond at the blob-blob junction. The rotation about the bonds joining the blobs has the capacity to change the overall dimensions of the blob chain.

The relationship between the observed results and the 'blob' model may be qualitatively explained in terms of the Kuhn and Grun model for the polarisable polymer chain. When a shear force is applied to the polymer system the polarisable persistence lengths will align in the shear direction. However, while the segment is aligned, the persistence length will remain unchanged with shear. A deficiency of the Kuhn and Grun model is that it does not take into account excluded volume effects. It is, therefore possible to improve the qualitative analysis of the Kuhn and Grun model by discussing the polarisable persistence length in terms of the blob diameter. While the overall thermodynamic motion of the blob chain is altered by a shear-induced deformation, the blob dimensions and persistence length remain constant with shear.

4. Conclusions

The random coil polymer p-4BCMU shows no measurable change in the distribution of conjugation lengths in the polymer backbone with shear. The data obtained in this study shows that there is no measurable change of the statistical segments describing the polymer backbone under shear. The Kuhn and Grun model, where the random coil is composed of polarisable segments, may be used in conjunction with the 'blob' model, to explain the observed spectroscopic data. Alignment of the blobs and polymer coils with the major axis parallel to the shear field increases the absorption cross-section in the flow direction, while reducing the absorption perpendicular to the shear field. The polymer chain persistence length, used in the molecular models describing dynamic polymer theory, is related to the backbone conjugation length and is shown to remain constant with shear. While the globular polymer coil changes conformation with shear, the polymer segment is oriented and the length remains unchanged during the overall coil deformation. This result is in agreement with kinetic theory, where a constant chain segment length is assumed for a change in the end-to-end distance of the polymer coil.

Acknowledgements

Sam Gason gratefully acknowledges the assistance of the Commonwealth Australian Postgraduate Award Scholarship (APA), and the Australian Research Council (ARC). The Advanced Minerals Product Research Centre, a Special Research Centre funded by the Australian Research Council supports part of this work.

References

[1] Lim KC, Heeger AJ. J Chem Phys 1985;82:522.
[2] Patel GN, Chance RR. J Polym Sci: Polym Lett Ed 1978;16:607.
[3] Patel GN, Yang NL. J Chem Edn 1983;60:181.
[4] Rughooputh SDDV. Syn Met 1996;80:195.
[5] Schott M, Wegner G. Nonlinear optical properties of organic molecules and crystals. Orlando: Academic Press, 1987.
[6] Xu R, Chu B. Acc Chem Res 1991;24:364.
[7] Lim KC, Fincher Jr. CR, Heeger A. J Phys Rev Lett 1983;50:1934.
[8] Allegra G, Bruckner S, Schmidt M, Wegner G. Macromolecules 1986;19:399.
[9] Chu B, Xu R. Acc Chem Res 1991;24:384.
[10] Peiffer DG, Chung TC, Schulz DN, Agarwal PK, Garner RT, Kim MW. J Chem Phys 1986;85:4712.
[11] Astakhova TY, Likhachev VN, Vinogradov GA. Chem Phys Lett 1991;184:81.
[12] Patel GN, Witt JD, Khanna YP. J Polym Sci: Polym Phys Ed 1980;18:1383.
[13] Wenz G, Muller MA, Schmidt M, Wegner G. Macromolecules 1984;17:837.
[14] Sakamoto K, Yoshida M, Sakurai H. Macromolecules 1994;27:881.
[15] Campbell AJ, Davies CKL. Polymer 1994;35:4787.
[16] Dobrosavljevic V, Stratt RM. Phys Rev B 1987;35:2781.
[17] Kuhn W. Kolloid-Z 1934;68:2.
[18] Bird RB, Curtis CF, Armstrong RC, Hassager O. Dynamics of polymeric liquids: Kinetic theory. New York: Wiley-Interscience, 1987.
[19] Rouse PE. J Chem Phys 1953;21:1272.
[20] Zimm BH. J Chem Phys 1956;24:269.
[21] Macosko CW. Rheology: Principles, measurements and applications. New York: VCH, 1994.

[22] Treloar LRG. The physics of rubber elasticity. London: Oxford University Press, 1958.
[23] Fuller GG. Optical rheometry of complex fluids. New York: Oxford University Press, 1995.
[24] Peterlin A, Heller W, Nakagaki M. J. Chem. Phys. 1958;28:470.
[25] Cottrell FR, Merrill EW, Smith KA. J Polym Sci: Polym Phys Ed 1969;7:1415.
[26] Link A, Springer J. Macromolecules 1993;26:464.
[27] Zisenis M, Springer J. Polymer 1994;35:3156.
[28] Lee EC, Solomon MJ, Muller SJ. Macromolecules 1997;30:7313.
[29] Lee EC, Solomon MJ, Muller S. J Polym Mat: Sci Eng 1997;77:592.
[30] Li L, Larson RG. Macromolecules 2000;33:1411.
[31] Bossart J, Ottinger HC. Macromolecules 1995;28:5852.
[32] Perkins TT, Smith DE, Chu S. Science 1994;264:819.
[33] Perkins TT, Quake SR, Smith DE, Chu S. Science 1994;264:822.
[34] Patel GN, Chance RR, Witt JD. J Chem Phys 1979;70:4387.
[35] Gason SJ, Dunstan DE, Smith TA, Chan DYC, White LR, Boger DV. J Phys Chem B 1997;101:7732.
[36] Taylor GI. Proc Roy Soc 1923;A105:541.
[37] Patel GN, Miller GG. J Macro Sci Phys 1981;B20:111.
[38] Kuhn H. Forts Chem Org Natur 1958;16:169.
[39] Kuhn H. Forts Chem Org Natur 1959;17:404.
[40] Kohler BE, Woehl JC. Syn Met 1997;84:851.
[41] Chance RR, Kiss AD, Peiffer DG, Hefner G, Pearson DS. Polym Mat: Sci Eng 1989;61:38.
[42] Pearson DS, Chance RR, Kiss AD, Morgan KL, Peiffer DG. Syn Met 1989;28:D689.
[43] Richards EG. An introduction to the physical properties of large molecules in solution. Cambridge: Cambridge University Press, 1980.
[44] Xu R, Chu B. Macromolecules 1989;22:3153.
[45] Lim KC, Kapitulnik A, Zacher R, Heeger AJ. J Chem Phys 1985;82:516.
[46] De Gennes PG. Scaling concepts in polymer physics. London: Cornell University Press, 1979.
[47] Dondos A. Polymer 1992;33:4375.
[48] Weill G, des Cloizeaux, J. J Phys 1979;40:99.
[49] Akcasu AZ, Benmouna M, Alkhafaji S. Macromolecules 1981; 14:147.
[50] Rieger J. Polymer 1998;39:4417.
[51] Duhamel J, Yekta A, Winnik MA, Jao TC, Mishra MK, Rubin ID. J Phys Chem 1993;97:13708.